Proceeding of the 2004 American Control Conference
Boston, Massachusetts June 30 - July 2, 2004

Underwater vehicle trajectory estimation using contracting PDE-based observers

Jérôme Jouffroy
Center for Ships and Ocean Structures (CESOS)
Norwegian University of Science and Technology (NTNU)
NO-7491 Trondheim, Norway
Email: jouffroy@marin.ntnu.no

Jan Opderbecke
Underwater Robotics, Navigation and Vision Department (RNV)
French Institute for Ocean Research (IFREMER)
83507 La-Seyne-sur-Mer, France
Email: Jan.Opderbecke@ifremer.fr

***Abstract*— This paper addresses the issue of estimating underwater vehicle trajectories using Gyro-Doppler (body-fixed velocities) and acoustic signals (earth-fixed positions). The approach consists of diffusion-based observers processing a whole trajectory segment at a time, allowing to consider important practical problems such as different information update rates, outages, and outliers in a very simple framework. Results of [10] are used to prove that the observers are contracting, *i.e.* convergent in the sense of contraction analysis. Simulation and experimental results are presented to illustrate the potential of application of the method.**

I. Introduction

Knowing precisely enough the horizontal position of an underwater vehicle evolving at the bottom of the sea is of great importance, not only for precise maneuvering and other control-based concerns, but also because the accurate knowledge of the vehicle trajectory is often the first step of other tasks or processing, whether they are done online (control purposes, marking interesting spots undersea...) or offline (cartography, video mosaicking,...)[13].
The precision of position sensing is however limited, depending on many different factors like for example the kind and type of sensors used (Doppler-gyrocompas, Long BaseLine (LBL), Ultra-Short BaseLine (USBL), Inertial Measurement Unit (IMU), ...) as well as the events that are often connected with the sensors features or environmental conditions like noise, sensor misalignment, outliers and outages (see [16], [15], [6] for an excellent review of the field).

This paper presents a new method for estimating the horizontal position of an underwater vehicle trajectory using principally Gyro-Doppler measurements (speed measurements) and an acoustic positioning system (horizontal position). The method is based on the use of Partial Differential Equations-based (PDE-based) observers that process whole segments of the vehicle trajectory. As it will be seen, one of the main advantages of such an approach is that, unlike other studies on navigation (see for example [1], [11], [12], [5], [2]), many of the difficulties subsequent to the Doppler-gyro / USBL combination (different information rates, Doppler-gyro drift, outliers, outages of the acoustic system,...) are treated very simply by starting with the same basic equations, thus leading to a quite unified view of the problem at hand.
The finite element approximations that are used to implement the observers are proven to be contracting, *i.e.* stable in the sense of *contraction analysis* [10] and therefore exhibit an exponential convergence.
Computer simulations and full-scale experiments on the deep sea ROV *Victor 6000* were carried out to demonstrate the observers performance. Some of these results are included in this paper.

The rest of the paper is organized as follows. After this introduction, a few elements of underwater vehicle navigation are given in section 2 in order to define the problem both theoretically and practically. In section 3, three PDE-based observers based on the diffusion equation are introduced. The first addresses the basic problem of combining Doppler-gyro speed measurements with USBL positions. The second one considers the use of time-constraints on the trajectory, *i.e.* different moments for which the vehicle was at the same position, after a loop-like trajectory. The above observers were designed for off-line purposes. The third subsection briefly addresses the important issue of online trajectory estimation taking the considered segments of trajectory as sliding along the latter and presents other possible extensions to the above observers. Experimental results are discussed in section 4. Brief concluding remarks end the paper.

II. Underwater vehicle navigation

As the problem that will be hereafter considered only addresses horizontal positioning, the kinematics can be written as follows [3]

$$\begin{pmatrix} \dot{x} \\ \dot{y} \end{pmatrix} = \begin{pmatrix} \cos\psi & -\sin\psi \\ \sin\psi & \cos\psi \end{pmatrix} \begin{pmatrix} u \\ v \end{pmatrix} \tag{1}$$

where the vector $(x, y)^T$ is the vehicle position with reference to an earth-fixed frame, ψ the heading given by a gyrocompass, and $(u, v)^T$ the vector of body-fixed velocities.
Note that by defining a complex setting $X = x + iy$ and $U = u + iv$, equation (1) is reduced to

$$\dot{X} = e^{i\psi} U \tag{2}$$

Fig. 1. IFREMER ROV Victor 6000

The above complex notation will be used in the rest of the paper. Hence, the positions given by the acoustic system (USBL or LBL) will be denoted as X_{ac}. From a practical standpoint, these measurements are typically corrupted by noise and can possibly suffer from a high percentage of outliers and outages. In addition to this, the update rate of the positioning information lies between 0.1 and $1Hz$, depending on the system in use.

The body-fixed velocities are measured by a bottom-lock Doppler sonar consisting of four downward-looking beam transducers used to the sea bottom. These velocities, noted V_{dop} can then be reinterpreted in the earth-fixed frame through the relation

$$V_{geo} = e^{i\psi} V_{dop} \tag{3}$$

where ψ is measured by the gyrocompass. V_{dop} and V_{geo} are typically less noisy than the acoustic positions and their refreshing rate are higher ($5Hz$ for the *Victor 6000* for example). However, integrating these velocities to obtain the vehicle trajectory (such a computation being referred to as dead-reckoning) can be not very accurate since the integration process creates a deviation caused for example by the accumulation of the small noise errors of the heading measurement [15].

III. Diffusion-based trajectory observers

By trajectory observers, it is meant that rather than estimating the current position of a vehicle, we are interested in the estimation of a whole trajectory segment. Formally, define $\hat{X}(s,t)$ the estimated trajectory as a continuous function of the trajectory time s, *i.e.* the temporal position along the trajectory, with $s \in [s_b, s_e]$ in seconds. The estimation process being iterative (*i.e.* it improves with iterations), let t represent the improvement time, with $t \in \mathbb{R}^+$, on which $\hat{X}$ also depends continuously.

The trajectory observers are based on the well-known diffusion equation [9] [8] [7]

$$\frac{\partial \hat{X}}{\partial t}(s,t) = \nabla^2 \hat{X}(s,t) \tag{4}$$

where $\nabla \hat{X} \triangleq \partial \hat{X} / \partial s$. This equation was proven to be contracting, *i.e.* incrementally stable in the sense of contraction analysis, provided Dirichlet boundary conditions are assumed. For more details on contraction analysis of partial differential equations, the reader is referred to [10].

In order to obtain a finite element implementation of (4), rewrite the Laplace operator in the following discrete approximation

$$\nabla^2 \hat{\mathbf{X}} = \frac{(n+1)^2}{S^2} \left(\begin{pmatrix} -2 & 1 & 0 & 0 & \ddots \\ 1 & -2 & 1 & \ddots & \ddots \\ 0 & 1 & \ddots & \ddots & 0 \\ 0 & \ddots & \ddots & -2 & 1 \\ \ddots & \ddots & 0 & 1 & -2 \end{pmatrix} \hat{\mathbf{X}} + \begin{pmatrix} \hat{X}_b \\ 0 \\ \vdots \\ 0 \\ \hat{X}_e \end{pmatrix} \right) \tag{5}$$

where n is the number of discrete elements of the trajectory segment, S is the segment length in seconds, and $\hat{X}_b$ and $\hat{X}_e$ are Dirichlet boundary conditions.

Proving that this implementation of (4) is contracting consists in verifying that the symmetric part of its Jacobian with respect to $\hat{\mathbf{X}}$, *i.e.*

$$\frac{\partial \nabla^2 \hat{\mathbf{X}}}{\partial \hat{\mathbf{X}}} = \frac{(n+1)^2}{S^2} \begin{pmatrix} -2 & 1 & 0 & 0 & \ddots \\ 1 & -2 & 1 & \ddots & \ddots \\ 0 & 1 & \ddots & \ddots & 0 \\ 0 & \ddots & \ddots & -2 & 1 \\ \ddots & \ddots & 0 & 1 & -2 \end{pmatrix} \tag{6}$$

is uniformly negative definite (u.n.d.), which is easy to check using Sylvester lemma. Such a discretizing process will be our main tool for checking the contracting behavior of the implementation of the trajectory observers.

From a trajectory point-of-view, the contracting behavior of the diffusion equation (4) means that for all initial estimated trajectory, the final estimation is unique provided Dirichlet boundary conditions are assumed, *i.e.* the extremum positions represented by the start and end points of the vehicle trajectory are known.

A. Velocity-guided diffusion observer

In order to combine appropriately the most interesting properties of the two measurements $V_{geo}(s)$ and $X_{ac}(s)$, we construct the following PDE-based trajectory observer

$$\frac{\partial \hat{X}}{\partial t} = \nabla(\nabla \hat{X} - V_{geo}(s)) + k_X(s)(X_{ac}(s) - \hat{X}) \quad (7)$$

where $V_{geo}(s)$ is introduced to guide the smoothing behavior of the diffusion-based filter according to the vehicle dynamics, and $X_{ac}(s)$, in feedback with $\hat{X}$, ensures that the final trajectory resembles the global positioning feature of $X_{ac}(s)$. Basically, the motivation of the above observer is that the final estimated trajectory $\hat{X}$ should be the result of a balance between a close match of $\hat{X}$ with X_{ac}, and another one of $\nabla \hat{X}$ with V_{geo} (see [13, section II.D.2]).

To take care of the acoustic signal, as well as its outliers and outages, the observer gain is defined as

$$k_X(s) = K \sum_{i=1}^{n_s} \delta(s - s_i) \quad (8)$$

where K is a strictly positive constant, $\delta(\cdot)$ stands for the Dirac delta function, and $s_i \in [s_b, s_e]$ are the trajectory times for which the acoustic signal is available. Hence, n_s is the number of available acoustic signals on the interval $[s_b, s_e]$. Note that such a framework allows to deal with a non-periodic acoustic signal which appears for example when many outages perturb the signal. Also, the outliers are treated as outages in the observer as they are simply discarded whenever detected.

once again, proving that the trajectory observer (7) is contracting is simple. Indeed, noting that $V_{geo}(s)$ and $X_{ac}(s)$ are just inputs to the observer, we can restrict the study of the combination of the Laplace operator (with Neumann boundary conditions)

$$\nabla^2 \mathbf{\hat{X}} = \frac{(n+1)^2}{S^2} \left(\begin{pmatrix} -1 & 1 & 0 & 0 & \ddots \\ 1 & -2 & 1 & \ddots & \ddots \\ 0 & 1 & \ddots & \ddots & 0 \\ 0 & \ddots & \ddots & -2 & 1 \\ \ddots & \ddots & 0 & 1 & -1 \end{pmatrix} \mathbf{\hat{X}} + \frac{S}{n+1} \begin{pmatrix} -\nabla \hat{X}_b \\ 0 \\ \vdots \\ 0 \\ \nabla \hat{X}_e \end{pmatrix} \right) \quad (9)$$

with the Dirac-based observer gain (8).

Thus, to show that the symmetric part of the discrete approximation of the Jacobian of $\nabla^2 \hat{X} - k_X(s)\hat{X}$ is uniformly definite negative, one has just to ensure that, in the case where only one acoustic measurement is available, the following matrix is uniformly positive definite.

$$\begin{pmatrix} 1 & -1 & 0 & 0 & \ddots & \ddots & 0 \\ -1 & 2 & -1 & \ddots & \ddots & \ddots & \ddots \\ 0 & -1 & \ddots & \ddots & \ddots & \ddots & \ddots \\ 0 & \ddots & \ddots & 2+K & -1 & \ddots & 0 \\ \ddots & \ddots & \ddots & -1 & \ddots & \ddots & 0 \\ \ddots & \ddots & \ddots & \ddots & \ddots & 2 & -1 \\ 0 & \ddots & \ddots & 0 & 0 & -1 & 1 \end{pmatrix} \quad (10)$$

Using Sylvester lemma and computing the principal minors of (10), it can be seen that $\Delta_i = 1$ for all i until $i = k$ the index of the available acoustic measurement for which $\Delta_k = 1 + K$. For $i > k$, $\Delta_i = 1 + (i - k + 1)K$. The last principal minor Δ_n, *i.e.* the determinant of (10) is then equal to K. Thus, all minors Δ_i are positive, hence (10) is uniformly positive definite, meaning that the discrete version of $\nabla^2 \hat{X} - k_X(s)\hat{X}$ is contracting, as well as the implementation of observer (7) with one acoustic measurement.

Using the fact that the sum of contracting systems is also contracting, contraction is then proven for the observer for any finite number of acoustic measurements.

Additionally, note that the above observer can be easily modified using a nonlinear diffusion term as follows

$$\frac{\partial \hat{X}}{\partial t} = \nabla f(\nabla \hat{X} - V_{geo}) + k_X(X_{ac} - \hat{X}) \quad (11)$$

Contraction can still be concluded for (11) provided one assumes some mild condition of linear bounded growth on f (see [9]). Indeed, one has

$$\nabla f(\nabla \hat{X} - V_{geo}) = \frac{\partial f}{\partial(\nabla \hat{X} - V_{geo})} \nabla(\nabla \hat{X} - V_{geo}) \quad (12)$$

B. Adding "rendez-vous" time constraints

Some missions of underwater vehicles consist of surveying a sea floor area for cartography and video-mosaicking purposes [13]. During these surveys, the path profiles are such that the vehicle happens to go over the same spot at two different times, thus creating loops (see figure 2). Such events being detected for example by cameras, meaning the actual position of the spot is not known, it is of interest to compensate the deviations due to noise on the Doppler sensor by using these "rendez-vous" time constraints in the case that only the extremum positions of the considered trajectory are known (see [2]).

The corresponding trajectory observer for a single-loop trajectory can be written as follows.

$$\begin{aligned} \frac{\partial \hat{X}}{\partial t} = \nabla(\nabla \hat{X} - V_{geo}) & \\ + k_L(\hat{X}(s_2, t) - \hat{X}(s_1, t))\delta(s - s_1) & \\ + k_L(\hat{X}(s_1, t) - \hat{X}(s_2, t))\delta(s - s_2) & \quad (13) \end{aligned}$$

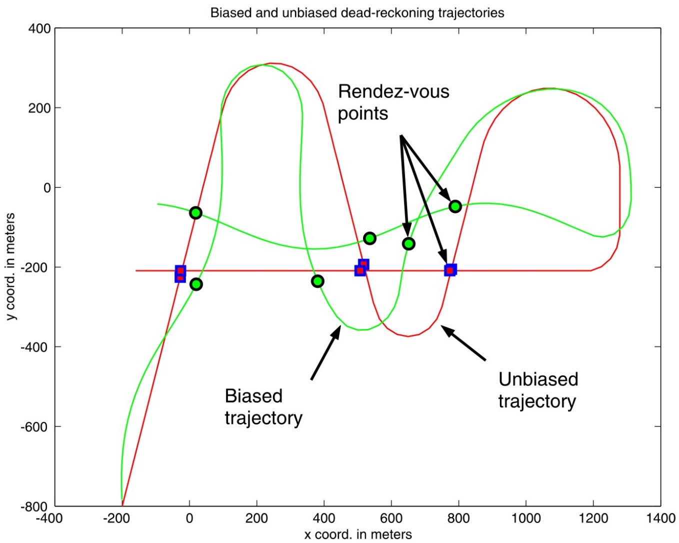

Fig. 2. Simulation of the unbiased and biased version of a three-loop trajectory

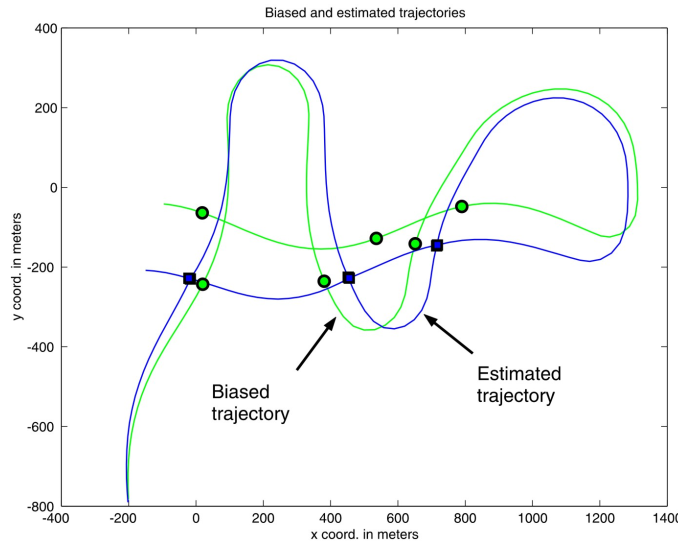

Fig. 3. The biased trajectory and its PDE-based correction

in which Dirichlet boundary conditions are assumed. k_L is a strictly positive constant, and s_1 and s_2 are the two trajectory times for which the positions are the same.

As for observer (7), checking the contraction property is not difficult if one uses the fact that observer (13) is contracting if the sum of the following matrices is u.n.d.

$$\begin{pmatrix} -2 & 1 & 0 & 0 & \ddots \\ 1 & -2 & 1 & \ddots & \ddots \\ 0 & 1 & \ddots & \ddots & 0 \\ 0 & \ddots & \ddots & -2 & 1 \\ \ddots & \ddots & 0 & 1 & -2 \end{pmatrix}$$

$$+ k_L \begin{pmatrix} 0 & 0 & \ddots & \ddots & \ddots & 0 \\ 0 & -1 & \ddots & \ddots & 1 & \ddots \\ \ddots & \ddots & 0 & \ddots & \ddots & 0 \\ \ddots & \ddots & \ddots & \ddots & \ddots & \ddots \\ \ddots & 1 & \ddots & \ddots & -1 & \ddots \\ 0 & \ddots & 0 & \ddots & \ddots & 0 \end{pmatrix} \qquad (14)$$

where the first matrix corresponds to the Jacobian approximation of the Laplace operator with Dirichlet conditions, and the second one, which are the terms induced by the observer feedback, stands for the rendez-vous time constraints.
It is straightforward to show that the latter matrix is uniformly semi-definite negative, and that this subsystem is therefore semi-contracting, while the former matrix is u.n.d according to [10]. The contraction property of (7) directly follows from the fact that the sum of a contracting system with a semi-contracting one is contracting.

In figure 2 is represented the simulation of a real trajectory (unbiased trajectory) of a vehicle and a Doppler-based version of it for which the Doppler sensor was highly corrupted by a slow noise (slow noise). The dots indicate the "rendez-vous" trajectory times as detected by a camera. It can be seen from the so-called biased trajectory that the error induced by the slow noise affects the rendez-vous constraints as each meeting point is quite distant from its counterpart (see the rendez-vous points pointed by the arrows). This problem is significantly corrected using a three-loop version of the above observer as shown in figure 3 where the rendez-vous constraints are recovered in the estimated trajectory.

C. Online version and further extensions

The trajectory observers that were hitherto depicted can be simply extended. For example, if instead of an off line trajectory observer (like the one in (7)) which is mainly useful in postprocessing tasks such as video mosaicking [13], a more real-time version of a trajectory observer would be

$$\frac{\partial \hat{X}}{\partial t} = \nabla(\nabla \hat{X} - V_{geo}) + v \nabla \hat{X} + k_X (X_{ac} - \hat{X}) \qquad (15)$$

where v accounts for the speed at which the trajectory segment to be estimated is moving in time along the whole trajectory. This observer is in turn contracting since the additional term $\nabla \hat{X}$ has been shown to have no effect on the contraction behavior in [10].
In figure 4 is represented the simulation of such an observer for a one-dimensional trajectory, for which the observer was not initialized on the exact location of the real trajectory. As in a usual Luenberger observer, the trajectory observer recovers the actual trajectory after a transient. The 3D view of figure 5 illustrates the sliding trajectory segment aspect of the same simulation.

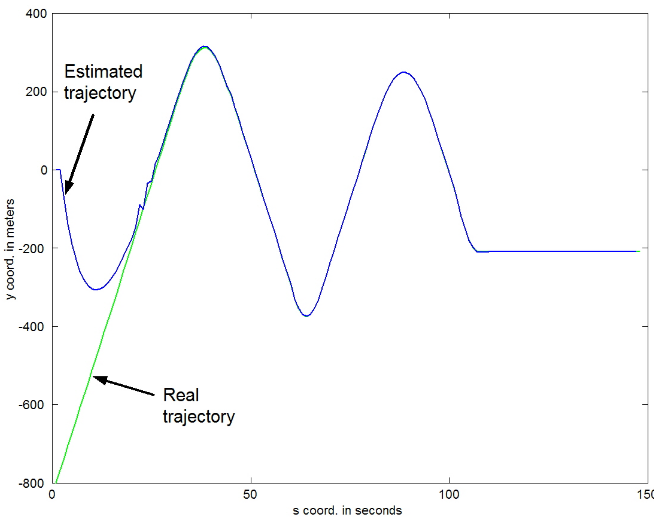

Fig. 4. Simulation of observer (15) for a one-dimensional trajectory

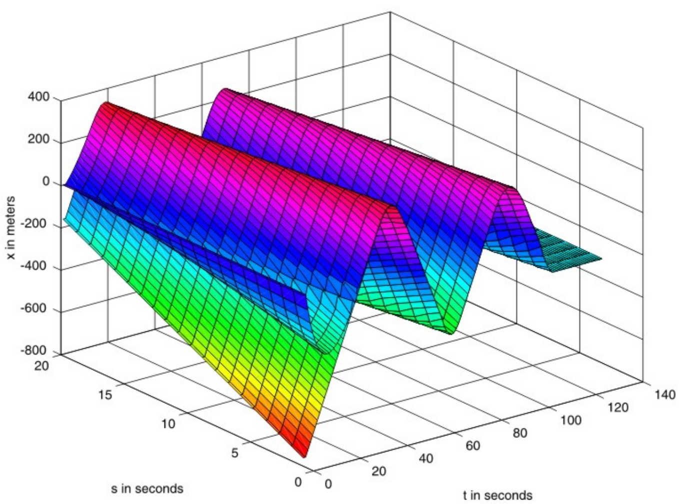

Fig. 5. 3D representation of the simulation of observer (15)

In the case where there are also outages on the Doppler signal, observer (7) can be augmented and rewritten as

$$\frac{\partial \hat{X}}{\partial t} = \nabla(\nabla \hat{X} - \hat{V}) + k_X(X_{ac} - \hat{X}) \quad (16)$$
$$\frac{\partial \hat{V}}{\partial t} = \nabla^2 \hat{V} + k_V(V_{geo} - \hat{V}) \quad (17)$$

where equation (17) takes care of the outages of V_{geo} in the same way as it is done in (16) for X_{ac}.
The overall contracting behavior of observer (16)-(17) is then easily concluded by using the combination result of contracting systems in cascade form.

Finally, if some acceleration measurements are added to the available information, equation (17) can be in turned changed into

$$\frac{\partial \hat{V}}{\partial t} = \nabla(\nabla \hat{V} - A_{ins}) + k_V(V_{geo} - \hat{V}) \quad (18)$$

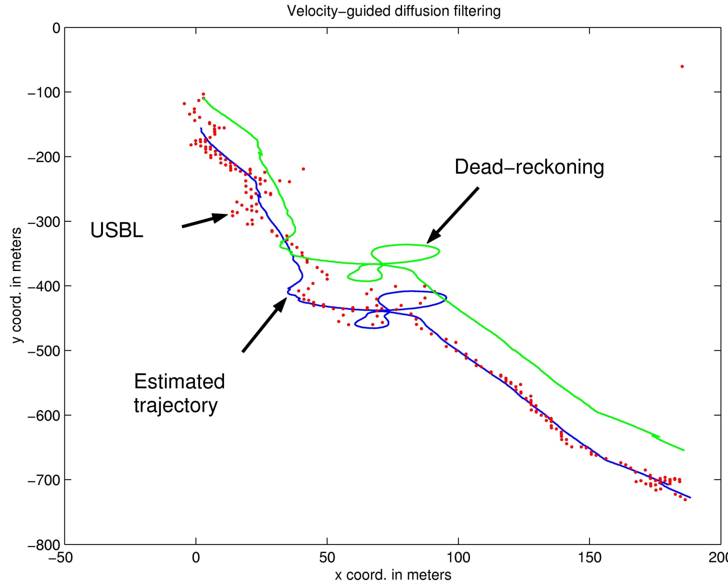

Fig. 6. Experimental result of the velocity-based diffusion-observer (7)

EXPERIMENTAL RESULTS

Full-scale test trials have been performed at sea during the joint IFREMER-AWI "Victor in the North" scientific cruise in the Atlantic ocean. Figure 6 shows one result of the combination of the USBL acoustic positioning system data of Victor 6000 with its Gyro-Doppler measurements using trajectory diffusion-based observer (7) which was implemented in Matlab code using AOS schemes for diffusion-based algorithms [14].
The starting point of the trajectory is in the upper left corner of the plot. The acoustic pings of the USBL system are easily spotted. Note the outlier in the upper righthand corner. The dead-reckoning trajectory is obtained after integration of the Gyro-Doppler data. This dead-reckoning process is initialized at the beginning of the trajectory.
The reader will certainly notice the differences between these two curves. The acoustic-based one has a good global position which is however noisy and not smooth, while the Gyro-Doppler trajectory behaves nicely regarding the dynamical aspects but is "bent" by error on the integration process.

On the practical point-of-view, note that these two trajectories are the main information that are available to the operational team and pilots of Victor 6000 to know the horizontal location and trajectory of the vehicle. In order to reduce the mismatch between the two trajectories, the initial value of the Doppler-based trajectory is manually re-initialized every now and then, which creates steps in the trajectory that

do not correspond to realistic underwater vehicle dynamics and can therefore be unsuitable for cartography purposes.
The estimated trajectory is the result of the PDE-based filtering. Note the good aspect of this trajectory as it advantageously combines the smooth speed feature of the Gyro-Doppler measurements with the absolute positioning of the acoustic system.

IV. Concluding remarks

In this paper, a simple and reliable framework for estimating horizontal underwater vehicle trajectories was presented, consisting in processing a whole trajectory segment at a time using a diffusion-based observer which inputs are Gyro-Doppler measurements and acoustic signals.
Current research focus on extension of the above-described work to study important underwater vehicle navigation aspects such as gyrocompass bias estimation, sound velocity adaptive estimation as well as acoustic rangemeter positioning applications.
Also, combining statistic with diffusion filtering as in [4], finding an appropriate function f for the nonlinear observer (11) to improve the results if a subject of current study.

Acknowledgments

This work benefited from many interesting discussions with the pilots of Victor 6000, as well as useful comments and remarks from Ole Morten Aamo.

References

[1] P. E. An, A. J. Healey, J. Park, and S. M. Smith, "Asynchronous data fusion for AUV navigation via heuristic fuzzy filtering techniques," in *Proc. IEEE Oceans'97*, 1997, pp. 397–402.

[2] M. Borgetto, C. Jauffret, and V. Rigaud, "Auto-localisation d'un véhicule sous-marin exploratoire quadrillant une zone," in *Proc. GRETSI '03*, Paris, France, 2003.

[3] T. I. Fossen, *Guidance and control of ocean vehicles*. John Wiley & Sons, 1994.

[4] A. B. Hamza, H. Krim, and G. B. Unal, "Unifying probabilistic and variational estimation," *IEEE Signal Processing Magazine*, vol. 19, no. 5, pp. 37–47, 2002.

[5] J. Jouffroy, "A relaxed criterion for contraction theory: application to an underwater vehicle observer," in *European Control Conference*, Cambridge, UK, 2003.

[6] J. C. Kinsey and L. L. Whitcomb, "Towards in-situ calibration of gyro and doppler navigation sensors for precision underwater vehicle navigation," in *Proc. IEEE Int. Conf. on Robotics and Automation*, Washington, DC, 2002.

[7] D. Kristiansen, "Modeling of cylinder gyroscopes and observer design for nonlinear oscillations," Ph.D. dissertation, Dep. Eng. Cybernetics, NTNU, Trondheim, Norway, 2000.

[8] W. Lohmiller and J.-J. E. Slotine, "Global convergence rates of nonlinear diffusion for time-varying images," in *2nd Int. Conf. on Scale-Space Theories in Computer Vision*, Corfu, Greece, 1999.

[9] ——, "On stability of nonlinear reaction-diffusion processes," in *European Control Conference*, Karlsruhe, Germany, 1999.

[10] ——, "Stability analysis and observer design for nonlinear diffusion processes," in *New trends in nonlinear observer design*, Nijmeijer. H. and Fossen. T. I., Eds. Springer-Verlag, 1999, pp. 93–111.

[11] P. Oliveira and A. Pascoal, "Navigation systems design: an application of multi-rate filtering," in *Proc. IEEE Oceans'98*, 1998, pp. 1348–1353.

[12] B. Vik and T. I. Fossen, "A nonlinear observer for GPS and INS integration," in *Proc. IEEE Conf. on Decision and Control*, Orlando, Florida USA, 2001.

[13] A. G. Vincent, N. Pessel, M. Borgetto, J. Jouffroy, J. Opderbecke, and V. Rigaud, "Real-time geo-referenced video mosaicking with the MATISSE system," in *Proc. IEEE Oceans'03*, San Diego, CA, 2003.

[14] J. Weickert, B. M. ter Haar Romeny, and M. A. Viergever, "Efficient and reliable schemes for nonlinear diffusion filtering," *IEEE Transactions on Image Processing*, vol. 7, no. 3, pp. 398–410, 1998.

[15] L. L. Whitcomb, D. R. Yoerger, and H. Singh, "Advances in Doppler-based navigation of underwater robotic vehicles," in *Proc. Int. Conf. on Robotics and Automation*, Detroit, Michigan, 1999.

[16] ——, "Combined Doppler / LBL based navigation of underwater vehicles," in *Proc. Int. Symposium on Unmanned Untethered Submersible Technology*, Durham, New Hampshire, 1999.